

Emergence of a hump in the cubic dielectric response of glycerol: a MD study

Marceau Hénot^{1,*} and François Ladieu¹

¹*SPEC, CEA, CNRS, Université Paris-Saclay, CEA Saclay Bat 772, 91191 Gif-sur-Yvette Cedex, France.*

(Dated: October 2, 2024)

We report a direct determination of the cubic dielectric spectra of a realistic polar molecule, glycerol, from molecular dynamic (MD) simulations. From the liquid state to the mildly supercooled regime, we observed the emergence and growth of a hump in the cubic modulus, traditionally associated with collective effects in the dynamics. Its evolution follows that of dynamical correlations probed by the four-point susceptibility and its apparition at high temperature coincides with the onset of super-activation. We show that, for this system, the shape of cubic spectra is only weakly affected by dipolar cross-correlations. The good agreement with experimental observations, despite the difference in temperature range, demonstrates the relevance of this approach to help get an insight into the intricate effects probed by non-linear dielectric spectroscopy.

The cooling of a supercooled liquid is associated with a dramatic slow-down of its structural relaxation time, ultimately leading to a virtually arrested out-of-equilibrium state called a glass [1]. This phenomenon is accompanied by an increasingly spatially correlated dynamics, as demonstrated experimentally [2–4] and numerically [5–7]. However, its physical origin and whether or not it is a sign of collective relaxation is still an ongoing question [8–11].

The precise experimental characterization of the correlated dynamic is a challenge. One popular technique in the literature is non-linear dielectric spectroscopy which focuses on the response of a polar liquid to a large electric field. While applying a tiny ac field allows to probe its reorientational dynamics in a non-perturbative way, a large field, by displacing the equilibrium state [12], gives access to rich and original information regarding cross-correlation effects [13–15], the out-of-equilibrium response to the perturbation [16, 17] or the collective nature of the relaxation [4, 18–23]. The later effect was predicted to be associated with the presence of a hump in the non-linear modulus, which grows upon cooling [24], a feature recently observed also in non-linear shear-mechanical experiments [25]. Non-linearities can be probed in different ways: a large ac field at frequency f has cubic contributions at f and $3f$ [4, 14] displaying slightly different spectra [18, 22]. Alternatively, applying a large dc field E_0 leads to a change in the linear response $\chi_1(f)$ quadratic in E_0 [15, 20, 22, 26–29]. This method has the advantage of not being subject to the heating effect induced by a large ac field. The associated complex cubic susceptibility $\chi_{2,1}$ can be defined as [20]:

$$\chi_{2,1}(f) = \frac{1}{2 \times 3} \frac{\partial^2 \chi_1(f)}{\partial E_0^2} \quad (1)$$

The main limitations of non-linear dielectric spectroscopy lie in its delicate interpretation as well as in the experimental challenge of measuring weak non-linear contributions, preventing measurements at $f > 50$ kHz.

MD simulations have been exploited to access the non-linear behavior of liquids, by applying a large ac electric field [30, 31] or, in static, through the statistics of the polarization at zero-field [32–35]. Yet, no cubic spectra comparable to experiments have been extracted.

In this letter, we report the first direct computation of the non-linear dielectric response $\chi_{2,1}(f)$ from a 3D MD simulation of glycerol, a system widely studied experimentally. We observed the apparition and growth upon cooling of the characteristic hump in the cubic modulus which compares well with experimental observations despite the difference in accessible temperature range. We take advantage of the numerical approach to study the effect of cross-correlations on the cubic response. Finally, we discuss how these results could help characterize the collective nature of the dynamics.

The simulations were carried out in the NPT ensemble on a system of $N = 2160$ glycerol molecules as in ref. [36] with a force field previously employed in the literature [37–40]. A static electric field E_0 was applied along one direction of the simulation box with an amplitude characterized by a dimensionless coefficient $\xi_0 = \mu E_0 / (k_B T)$ where k_B is the Boltzmann constant and $\mu = 3.2$ D is the mean molecule dipole. Care was taken to reach equilibrium at each temperature and field with an equilibration run of at least 100 times the self dipole relaxation time τ_{self} before a simulation run of at least $200\tau_{\text{self}}$. The total dipole correlation function is defined as:

$$C_{\text{tot}}(t) = \frac{1}{N} \left\langle \sum_i \sum_j \vec{\mu}_i(t_0) \cdot \vec{\mu}_j(t_0 + t) \right\rangle_{t_0} \quad (2)$$

It can be separated into a self part $C_{\text{self}}(t)$ for which $i = j$ and a cross part $C_{\text{cross}}(t)$ corresponding to $i \neq j$ [41].

The effect of E_0 on the self and total correlation functions is shown in fig. 1a at $T = 263$ K which is the lowest temperature that we simulated. Increasing E_0 has qualitatively the same effect on both the self and total correlation: The static values $C_{\text{self}}(0)$ and $C_{\text{tot}}(0)$ decrease and the relaxation times τ_{self} and τ_{tot} (with $\tau = \int C(t)/C(0)dt$) increase. For small enough field amplitude, it is expected that any effect should be propor-

* Corresponding author: marceau.henot@cea.fr

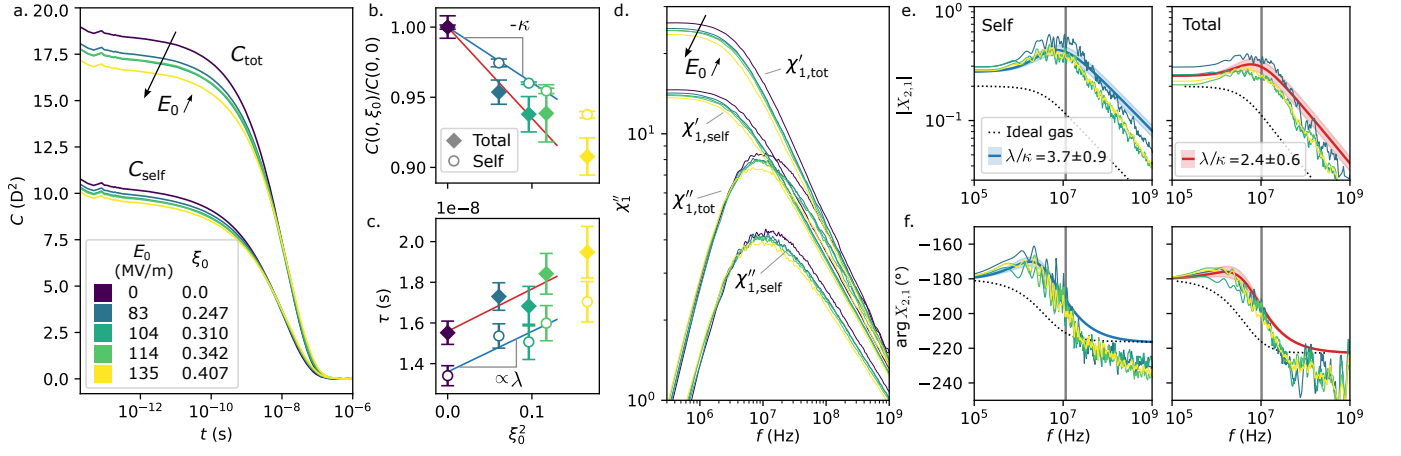


FIG. 1. (a) Dipole correlation function for the self and total cases at $T = 263$ K, in the presence of a static electric field characterized by $\xi_0 = \mu E_0 / k_B T$. (b) Static correlation and (c) relaxation time as a function of ξ_0^2 . Solid lines are linear fits for $\xi_0 < 0.35$. (d) Real and imaginary parts of the self and total linear spectra χ_1 . (e) Modulus and (f) phase of the cubic susceptibility $X_{2,1}$ for the self part (left) and total (right). Thin lines were obtained directly from the linear spectra. Blue and red thick lines correspond to the $\text{HN}_{\kappa,\lambda}$ method. The ideal gas of dipoles is shown with a dotted line.

tional to ξ_0^2 , which is the first non-zero order of the Taylor development for symmetry reasons:

$$\frac{C(0, \xi_0)}{C(0, 0)} \approx 1 - \kappa \xi_0^2 \quad \frac{\tau(\xi_0)}{\tau(0)} \approx 1 + \lambda \xi_0^2 \quad (3)$$

These relations are tested in fig. 1b and c, and appears valid within the uncertainty for $\xi_0 < 0.35$ ($E_0 < 114 \text{ MV}\cdot\text{m}^{-1}$, only twice larger than highest experimental fields [42]).

The complex linear susceptibility $\chi_1 = \chi_1' - j\chi_1''$ obtained from the Fourier transform of the correlation function (see appendix A) is shown in fig. 1d. The decrease of the static susceptibility $\chi_1'(0)$ and of the peak frequency of χ_1'' are well visible for the self and total cases. For small enough ξ_0 , the non-linear susceptibility $\chi_{2,1}$ can be approximated by the difference of the linear response in the presence and absence of field:

$$\chi_{2,1}(f) \approx \frac{1}{3} \frac{\chi_1(f, E_0) - \chi_1(f, 0)}{E_0^2} \quad (4)$$

The non-linear spectra can be expressed in a dimensionless form [20, 22] $X_{2,1}(f) = \chi_{2,1}(f) k_B T / (\chi_1(0)^2 \epsilon_0 v)$, where v is the molecular volume, constructed to be temperature independent for non-interacting dipoles (see below). The modulus and phase of $X_{2,1}$ for the self and total cases are shown in fig. 1e and f. They display the characteristic hump near $f_\alpha = 1/(2\pi\tau_{\text{tot}})$ observed experimentally in the deeply supercooled regime [20, 22].

To reduce the noise in the determination of $X_{2,1}(f)$, we use another approach, denoted in the following as $\text{HN}_{\kappa,\lambda}$ and analogous to the one introduced in refs. [15, 26–29]. It relies on the assumption that $\chi_{2,1}$ results from two main effects: a decrease in static susceptibility ($\kappa > 0$) and an increase in relaxation time ($\lambda > 0$). Additionally, the linear response is assumed to be described by

a Havriliak–Négyami expression (see Appendix B) whose parameters α and γ are fitted on the linear spectra in the absence of field and assumed independent of it. In this framework, the presence of a hump on $|\chi_{2,1}(f)|$ and its amplitude are controlled by the ratio λ/κ . It exists only if λ/κ is larger than a critical value close to 0.5 (see fig. A1). The resulting spectra are shown in fig. 1e and f and compare very well to the one obtained from the direct method, especially regarding the hump amplitude. The main difference concerns the high-frequency flank and is likely due to the assumption that γ is independent of E_0 . In the following, we use this second method, as it reduces the uncertainty on the peak value of the modulus.

We now turn to the effect of the temperature on the cubic spectra of glycerol, which we studied between 393 K and 263 K. The decrease in the static susceptibility with E_0 , characterized by κ , appears to follow an inverse power-law temperature dependence (see fig. A2) and is systematically higher for the total case than for the self by approximately 50 %. In contrast, the effect of E_0 on the relaxation time is strongly affected by the temperature, as shown in fig. 2a and b. It is smaller than the resolution at 393 K ($\lambda < 0.2$) and increases significantly upon cooling, reaching $\lambda = 1.5$ at 263 K.

The ratio λ/κ is shown in fig. 4d and the resulting moduli $|X_{2,1}|$ are displayed (up to a vertical prefactor for readability) in fig. 2c and d for the self and total cases respectively. The feature standing out is the apparition and growth of a hump when the temperature is decreased. This effect can be quantified through the maximum of the modulus shown in fig. 3c. The static value $|X_{2,1}(0)| = \mu^2 \kappa / (3k_B T \epsilon_0 v \chi_1(0))$ is shown in fig. 3b and appears almost temperature independent, close to 0.2 for the total case while it slightly decreases with T for the self case.

The present work is, to our knowledge, the first di-

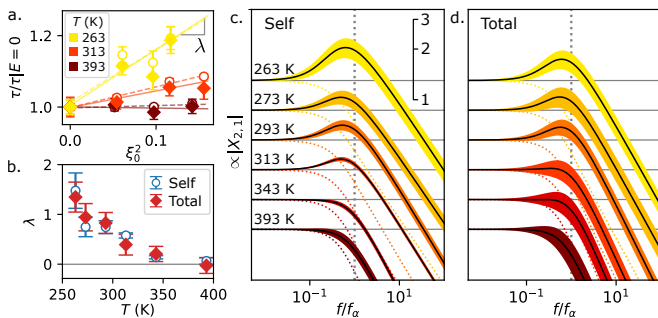


FIG. 2. (a) Effect of E_0 on the relaxation time for three temperatures. Dashed and solid lines are linear fits for the self and total cases respectively with slopes λ shown in (b) for all temperatures. (c-d) Modulus $|X_{2,1}|$ (from $\text{HN}_{\kappa,\lambda}$) in log-log scale at different temperatures for the self (c) and total (d) cases. The uncertainty related to the determination of λ/κ is shown. The curves are vertically shifted for readability.

rect 3D MD simulation of the dielectric non-linear spectrum of a molecular liquid. For the present system, glycerol, the cubic response has been measured extensively [20, 22, 26], and it is natural to directly compare these simulations with experimental observations. The moduli of $|X_{2,1}|$ obtained from refs. [20, 22] are shown with markers in fig. 3a. The static and maximum values, as well as the ratio λ/κ deduced from experiments of refs. [20, 22, 26] (see appendix D) are shown in fig. 3b, c and fig. 4d. In a dielectric experiment, the self and cross part cannot be separated and they should be compared to the MD total case. The range of accessible temperature in MD and experiments differs, the former being constrained by computational cost to $f > 1$ MHz while the latter is limited to $f < 50$ kHz. Still, the following points can be highlighted: (i) The static value $|X_{2,1}(0)|$ is independent of temperature and close to 0.2 in both total MD and experiments (see fig. 3b). (ii) The hump grows consistently when the temperature is decreased. This is particularly visible in fig. 3c where experimental and MD data align very well. (iii) In the $\text{HN}_{\kappa,\lambda}$ method, the hump is controlled by the ratio λ/κ and there again we see on fig. 4d a very good alignment. As a consequence, combining MD and experiments allows to access, at least qualitatively, the evolution of the cubic spectra on a wide temperature range, from the liquid regime down to the glass transition. Some features are however not perfectly reproduced in the simulations. The amplitude of cross-correlations is underestimated which makes the linear dielectric response $\chi_1(0)$, and thus $\chi_{2,1}(0)$, approximately 35-40 % smaller than in experiments. The slope of the high-frequency flank of $|X_{2,1}(f)|$ is slightly smaller than in experiments as it is already the case on the linear spectra [36]. This is not surprising as MD models usually have to be fitted specifically to reproduce dielectric quantities [43] which is not the case here. Also, given the long time windows required, the model had to be kept fairly simple and electronic polarizability was not taken into account. Finally, the non-linear dielectric

response of glycerol to a low frequency ($f < 20$ kHz) ac field has recently been reported to display a strong increase for $T > 280$ K [44]. This is in contrast with the almost temperature-independent $|X_{2,1}|(0)$ that we observed. This discrepancy may be related to the difference in non-linear observable (ac vs dc field) or to the fact that we are limited to frequencies not smaller than $10^{-2}f_\alpha$ while the increase was observed well below.

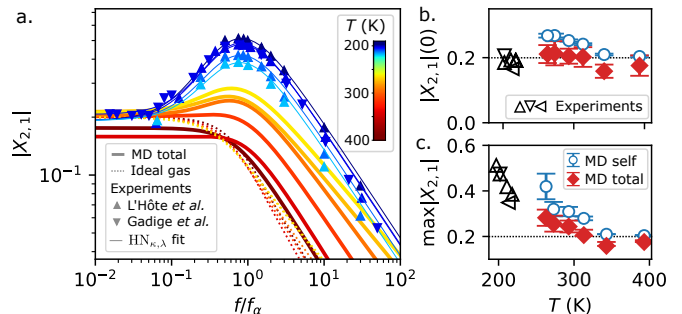


FIG. 3. (a) Cubic modulus for the total MD case (thick lines) and from experiments [20, 22] (markers). Thin lines correspond to a fit with $\text{HN}_{\kappa,\lambda}$. (b) Static value and (c) maximum of the modulus for the MD self and total cases and from experiments [20, 22, 26] (see legend in fig. 4b).

Beyond these limitations, a strong point of this MD approach is that it gives access to both the self and cross parts. The interpretation of dielectric spectroscopy is complicated by the presence of the cross part whose dynamics differs from the self [36, 45–48]. Here, we can disentangle these effects for the cubic response and we can conclude that, for glycerol, the cross part has only a weak effect on the non-linear spectra. Indeed, the shift in relaxation time is not modified at all and the change in static susceptibility, while increasing, keeps the same temperature dependence. Overall, as visible in fig. 3, the hump is only slightly more pronounced for the self than for the total. This confirms the pertinence of the cubic response in providing information on the molecular dynamics in itself for glycerol, independently of the dipole correlations. However, this is not necessarily true in general, and in some other systems, the cubic response appears to be dominated by the effect of cross-correlations [15, 29, 35].

To investigate collective effects in the molecular dynamics, cubic spectra can be compared to the case of an ideal gas of dipoles (*i.e.* without interactions) [49]. Consistently with the literature [21, 23], we computed the cubic response $\chi_{2,1}^{\text{id}}$ of an ideal gas having the same linear response than the considered system (see appendix E). These spectra are shown as dotted lines in fig. 1e-f, 2c-d and 3a. Starting from $|X_{2,1}^{\text{id}}(0)| = 1/5$ very close to experimental and MD results, the modulus is strictly decreasing and systematically lower than $|X_{2,1}|$. The collective nature of the dynamics can be characterized through the maximum of $|X_{2,1}(f) - X_{2,1}^{\text{id}}(f)|$ [21, 23]. This quantity has the advantage of being sensitive to small deviations from non-interacting dipoles, which is

particularly interesting in the high-temperature regime accessed here. It is shown in fig. 4a as a function of the inverse temperature for the present MD results and for experiments [20, 22, 26], and in fig. 4b as a function of the relaxation time. The MD self and total follow qualitatively the same ten-fold increase between 393 K and 263 K. In the experimental window, the increase is much weaker: 40 % between 218 K and 198 K. Here again, despite the difference in temperature range, the MD total and experimental data seem perfectly compatible.

A strength of these MD simulations is to give access to the high-temperature regime, not experimentally accessible. This enables us to observe the emergence of a hump in the cubic modulus between 343 K and 313 K. As mentioned above, a hump appears if λ/κ exceeds a critical value. The parameter κ , characterizing the static response, does not strongly depend on temperature, and it is the field-induced slow-down of the dynamic λ (also called electrorheological effect [27]), that, by appearing between 393 and 343 K, controls the emergence of the hump. Remarkably, it is in this same range, that the liquid goes from an Arrhenian dynamics with a constant activation energy E_∞ to a super-activated behavior with an activation energy $E_a(T)$ increasing with temperature [51, 52]. This is shown in fig. 4c which displays the ratio $E_a(T)/E_\infty$. It reaches a plateau for $T > T_o = 375 \pm 10$ K, the onset temperature.

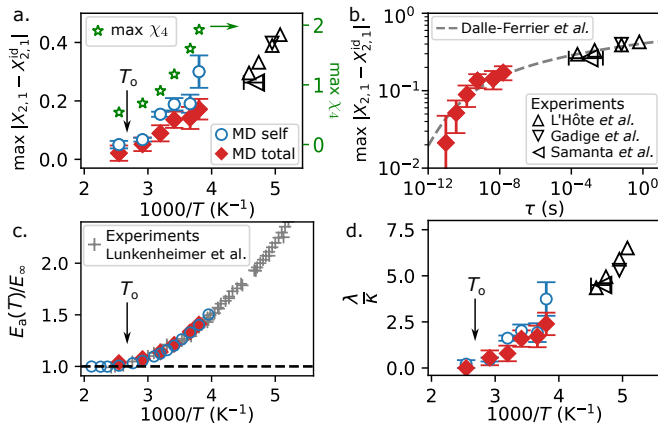


FIG. 4. (a) Maximum of $|X_{2,1} - X_{2,1}^{\text{id}}|$ as a function of the inverse temperature, for the MD self and total cases and from experiments [20, 22, 26]. Maximum of χ_4 (right vertical scale). (b) Same, as a function of the relaxation time. The dashed gray line is taken from ref. [53]. (c) Ratio of the activation energies at T and above the onset temperature T_o ($E_\infty = 22.5 \text{ kJ}\cdot\text{mol}^{-1}$) from MD and experiments [54] and (d) ratio λ/κ , as a function of the inverse temperature.

Different theoretical approaches were suggested to explain the physical origin of super-activation. Some are based on a purely dynamical transition induced by kinetic constraints [55, 56] in which the energy landscape is irrelevant. Others rely on facilitation caused by elastic stress redistribution following a local rearrangement [57–59]. Finally, theories based on thermodynamics put for-

ward the role of the complex free energy landscape whose minima would correspond to an *amorphous order* over a scale that grows upon cooling. In this case, relaxation events are not only spatially correlated but collective in nature [60, 61]. It is in this framework, that Bouchaud and Biroli [24] conjectured a growing hump in the cubic response of liquids, accompanying an increasingly collective dynamics, before it was ever measured [4, 18–22]. This link is not obvious *a priori* and propositions were made to interpret it without explicitly introducing collective effects [62, 63]. Yet, two angles can help get a qualitative understanding of it: (i) the concept of ‘superdipole’, *i.e.* an assembly of N_{corr} dipoles relaxing in a collective manner [10], leads to a hump growing with N_{corr} [64, 65]. (ii) The change of entropy induced by E_0 [12, 27], together with the Adam-Gibbs relation (linking τ and the configuration entropy S_c) leads to $\lambda \propto 1/S_c^2$. As increasing N_{corr} corresponds to decreasing S_c , it leads to a growing hump [22]. From another perspective, dynamical correlations in MD simulations can be directly characterized through the maximum of the four-point susceptibility $\chi_4(t)$ [7, 50] (see Appendix F) and is shown in fig. 4a with green stars. It appears to follow well the increase in cubic response, consistently with the idea that collective effects should imply dynamical correlations. Overall, the fact that the cubic modulus is not a direct characterization of correlations, but requires a collective behavior, can be seen as a strength, as it could help get information on the physical origin of super-activation. Indeed, it was recently shown by one of us that, on a 1D model glassformer, the correlated dynamics leads to a humped cubic modulus only when encoded into the Hamiltonian but not when coming from purely dynamical rules [66].

The dashed grey line in fig. 4b, reproduced up to a vertical prefactor from ref. [53], is designed to qualitatively describe the evolution of N_{corr} as predicted by an activated phenomenon close to the glass transition and by mode-coupling theory at shorter relaxation times. We see that $\max |X_{2,1} - X_{2,1}^{\text{id}}|$ follows well this curve and that the two regimes are well visible. This is consistent with a recent suggestion that, in a mildly supercooled liquid, the dynamic is controlled by entropy barriers as the free-energy landscape progressively gets more tortuous upon cooling. It is only below the mode-coupling temperature that the barriers will become of energetic nature [67]. Conversely, in the high-temperature regime $T > T_o$ of constant activation energy E_∞ the cubic response is close to the ideal gas one. This onset temperature is higher than the fusion temperature of glycerol (292 K) suggesting that the progressive evolution of the free-energy landscape, eventually leading to the dynamical arrest at low temperature, starts well in the liquid regime [68].

In this letter, we have shown that the cubic spectrum of a realistic polar liquid, here glycerol, could be obtained from MD simulations. We observed upon cooling the emergence of the characteristic hump in the cubic mod-

ulus reported experimentally and considered a signature of the collective nature of the dynamics. The MD results appear consistent with experimental measurements on the same system despite the difference in temperature range, which justifies the approximations made in the simulation. This numerical approach revealed that, in the case of glycerol, cross-correlations do not affect much the shape of the cubic spectra. Moreover, it appears that the emergence of the cubic hump is associated with the apparition of the so-called electro-rheological effect at high temperatures which coincides with the onset of super-activation. The hump growth correlates well with a direct characterization of the correlated dynamic, suggesting the importance of collective effects. As non-linear dielectric susceptibilities of supercooled liquid are considered a crucial tool to distinguish between different theoretical approaches of the glass transition [69], we hope that, in the future, this approach could be useful in the delicate interpretation of this powerful experimental technique.

The authors are grateful to L. Berthier and C. Alba-Simionesco for fruitful discussions, to LABEX PALM, IRAMIS Institute and Paris-Saclay university for financial support.

Appendix A: Linear susceptibility. The complex linear susceptibility $\chi_1 = \chi_1' - j\chi_1''$ was obtained through the following procedure: the imaginary part $\chi_1''(f) \propto f \times \text{TF}(C(t))$ was computed from the Fourier transform TF of each correlation function using the fftlog algorithm adapted to log spaced data [70]. From this, $\chi_1'(f)$ was deduced using the Kramers-Kronig relations and the susceptibility was finally rescaled so that $\chi_1'(0) = C(0)/(2\epsilon_0 k_B T v)$. The present MD simulation uses Ewald summation to treat Coulomb interactions and the static permittivity $\epsilon(0) = 1 + \chi_1'(0)$ is related to the Kirkwood correlation factor g_K by [71, 72]:

$$\frac{(\epsilon(0) - 1)(2\epsilon(0) + 1)}{\epsilon(0)} = \frac{\mu^2 g_K}{\epsilon_0 k_B T v} \quad (\text{A1})$$

The static correlation function can be expressed as $C_{\text{tot}}(0) = \mu^2 g_K$. From this, $\chi_1'(0)$ is given by the root of a second order polynomial and its dependence on $C_{\text{tot}}(0)$ is not straightforward. In the case where $\chi_1'(0) \gg 1$, $\chi_1'(0)$ can be assumed proportional to $C_{\text{tot}}(0)$: $\chi_1'(0) \approx (\mu^2 g_K)/(2\epsilon_0 k_B T v)$ which is the expression used in the main text for the sake of simplicity. We have checked that the error introduced by this approximation is smaller than 3 %.

Appendix B: $\text{HN}_{\kappa,\lambda}$ method. The expression used to parameterize the linear spectra is:

$$\chi_{1,\text{HN}}(f, \xi_0) = \frac{\chi_1(0)(1 - \kappa \xi_0^2)}{(1 + [j2\pi f \tau(1 + \lambda \xi_0^2)]^\alpha)^\gamma} \quad (\text{A2})$$

Within this framework, the emergence of a hump in the cubic modulus can be studied as a function of the parameters λ , κ , α and γ . As shown in fig. A1, a hump is

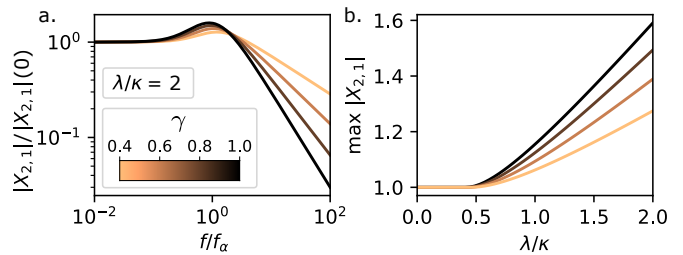


FIG. A1. (a) Cubic modulus from $\text{HN}_{\kappa,\lambda}$ for different high frequency slope controlled by the parameter γ . (b) Maximum of the modulus as a function of the ratio λ/κ .

present if the ratio λ/κ is larger than a critical value close to 0.5. The slope of the high frequency flank, controlled by γ , affects the growth of the hump with the ratio but has a negligible effect on the critical value.

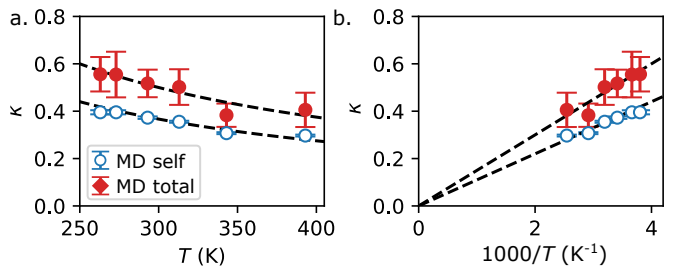


FIG. A2. Static cubic response parameter κ , as a function of temperature for the self and total cases. The black dashed lines correspond to $\kappa \propto 1/T$.

Appendix C: Static cubic response. The temperature dependence of the coefficient κ , characterizing the effect of the field on the static response, is shown in fig. A2 for the self and total case. It appears to follow an inverse temperature law (black dashed lines).

Appendix D: Comparison with experimental data. The modulus of $X_{2,1}$ from L'Hôte *et al.* [20] and Gadige *et al.* [22] were reproduced on fig. 3a and the ratio λ/κ was determined at each temperature by a fit with the $\text{HN}_{\kappa,\lambda}$ expression. Samanta and Richert [26] measured the effect of a static field $E_0 = 22.5 \text{ M}\cdot\text{V}^{-1}$ on the linear susceptibility $\chi_1(f)$. By fitting a Havriliak-Negami expression, they determined that between 208 and 227 K, the mean relaxation time was increased by $(\Delta\tau)/\tau = 2.7 \%$ and that the static susceptibility was reduced by $\Delta\chi_1(0)/\chi_1(0) = 0.6 \%$. The ratio of these two quantities is the same as the ratio $\lambda/\kappa = 4.5$. Besides, the static modulus can be computed from:

$$|X_{2,1}(0)| = \frac{1}{3} \frac{\Delta\chi_1(0)}{E_0^2} \frac{k_B T}{\chi_1(0)^2 \epsilon_0 v} \quad (\text{A3})$$

The maximum of $|X_{2,1}(f)|$ and of $|X_{2,1}(f) - X_{2,1}^{\text{id}}(f)|$ can be computed from λ/κ and the HN parameters given by the authors.

Appendix E: Ideal gas of dipoles. The cubic response to a static field of non-interacting dipoles for a Debye process is [49]:

$$\chi_{2,1}^{\text{id,D}}(x) = -\frac{1}{45} \frac{27 + x^2 - 2x^4 + jx(42 + 19x^2 + x^4)}{(1 + x^2)^2(9 + x^2)} \quad (\text{A4})$$

with $x = 2\pi f\tau$. The linear dynamics of the liquid can be decomposed on a basis of Debye functions and characterized by a distribution of relaxation time $G(\ln \tau)$ deduced, for example, from the HN fit [21]. The non-linear response $\chi_{2,1}^{\text{id}}(f)$ of an ideal gas of dipole that would have the same linear response $\chi_1(f)$ is [21, 23]:

$$\chi_{2,1}^{\text{id}}(f) = \int_{-\infty}^{\infty} \chi_{2,1}^{\text{id,D}}(2\pi f\tau) G(\ln \tau) d\ln \tau \quad (\text{A5})$$

It should be noted that to obtain $\chi_{2,1}^{\text{id}}$, the molecular re-orientation was modeled here by rotational diffusion but other frameworks can lead to a (T independent) humped shape for the modulus [73]. The fact that, at high temperature, $|\chi_{2,1}|$ does not display a hump and is very close to $|\chi_{2,1}^{\text{id}}|$ justifies the simple choice made here.

Appendix F: Four-point susceptibility. This quantity is defined by:

$$\chi_4(t) = \left\langle \sum_{j=1}^N c_i(t)c_j(t) \right\rangle_i - N \langle c_i(t) \rangle_i^2 \quad (\text{A6})$$

where $c(t)$ is a time correlation function chosen here to be the self dipole correlation: $c_i(t) = \vec{u}_i(t_0) \cdot \vec{u}_i(t_0 + t)$ with $\vec{u} = \vec{\mu}/\mu$. The result for each temperature is shown in fig. A3. It reaches its maximum close to the mean relaxation time and goes at long times to a plateau at $\approx 1/3$ related to the properties of the chosen correlation function. The maximum value for each temperature is shown with green stars in fig. 4a. Its increase upon cooling is a direct sign of increasingly correlated dynamics.

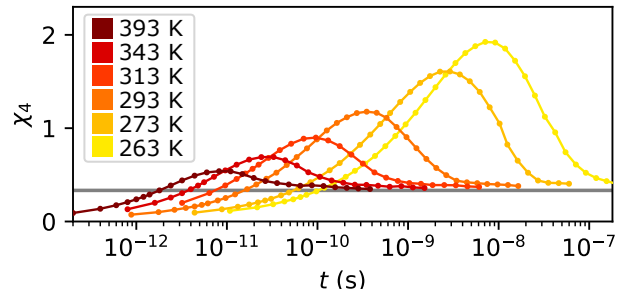


FIG. A3. Four-point susceptibility computed from the dipole correlation. The grey horizontal line corresponds to the long-time expected value of $1/3$.

-
- [1] C. A. Angell, K. L. Ngai, G. B. McKenna, P. F. McMillan, and S. W. Martin, *J. Appl. Phys.* **88**, 3113 (2000).
 - [2] E. Vidal Russell and N. Israeloff, *Nature* **408**, 695 (2000).
 - [3] S. Reinsberg, X. Qiu, M. Wilhelm, H. W. Spiess, and M. Ediger, *The Journal of Chemical Physics* **114**, 7299 (2001).
 - [4] C. Crauste-Thibierge, C. Brun, F. Ladieu, D. L'hôte, G. Biroli, and J.-P. Bouchaud, *Physical review letters* **104**, 165703 (2010).
 - [5] C. Donati, J. F. Douglas, W. Kob, S. J. Plimpton, P. H. Poole, and S. C. Glotzer, *Physical review letters* **80**, 2338 (1998).
 - [6] L. Berthier, *Physics Online Journal* **4**, 42 (2011), arXiv:1106.1739 [cond-mat.stat-mech].
 - [7] C. Scalliet, B. Guiselin, and L. Berthier, *Physical Review X* **12**, 041028 (2022).
 - [8] M. Wyart and M. E. Cates, *Physical review letters* **119**, 195501 (2017).
 - [9] L. Berthier, G. Biroli, J.-P. Bouchaud, and G. Tarjus, *The Journal of chemical physics* **150**, 094501 (2019).
 - [10] G. Biroli, J.-P. Bouchaud, and F. Ladieu, *The Journal of Physical Chemistry B* **125**, 7578 (2021).
 - [11] M. Pica Ciamarra, W. Ji, and M. Wyart, *Proceedings of the National Academy of Sciences* **121**, e2400611121 (2024).
 - [12] G. Johari, *The Journal of Chemical Physics* **138**, 154503 (2013).
 - [13] L. P. Singh and R. Richert, *Physical Review Letters* **109**, 167802 (2012).
 - [14] R. Richert, *Journal of Physics: Condensed Matter* **29**, 363001 (2017).
 - [15] J. P. Gabriel, E. Thoms, and R. Richert, *Journal of Molecular Liquids* **330**, 115626 (2021).
 - [16] R. Richert, J. P. Gabriel, and E. Thoms, *The Journal of Physical Chemistry Letters* **12**, 8465 (2021).
 - [17] R. Richert and J. P. Gabriel, *The Journal of Chemical Physics* **159**, 084504 (2023).
 - [18] C. Brun, F. Ladieu, D. L'Hôte, M. Tarzia, G. Biroli, and J.-P. Bouchaud, *Physical Review B* **84**, 104204 (2011).
 - [19] T. Bauer, P. Lunkenheimer, and A. Loidl, *Physical review letters* **111**, 225702 (2013).
 - [20] D. L'Hôte, R. Tourbot, F. Ladieu, and P. Gadige, *Physical Review B* **90**, 104202 (2014).
 - [21] R. Casalini, D. Fragiadakis, and C. Roland, *The Journal of chemical physics* **142**, 064504 (2015).
 - [22] P. Gadige, S. Albert, M. Michl, T. Bauer, P. Lunkenheimer, A. Loidl, R. Tourbot, C. Wiertel-Gasquet, G. Biroli, J.-P. Bouchaud, *et al.*, *Physical Review E* **96**, 032611 (2017).
 - [23] S. Albert, T. Bauer, M. Michl, G. Biroli, J.-P. Bouchaud, A. Loidl, P. Lunkenheimer, R. Tourbot, C. Wiertel-Gasquet, and F. Ladieu, *Science* **352**, 1308 (2016).
 - [24] J.-P. Bouchaud and G. Biroli, *Physical Review B* **72**, 064204 (2005).

- [25] K. Moch, C. Gainaru, and R. Böhmer, *The Journal of Physical Chemistry B* **128**, 8846 (2024).
- [26] S. Samanta and R. Richert, *The Journal of Chemical Physics* **142**, 044504 (2015).
- [27] S. Samanta and R. Richert, *The Journal of Physical Chemistry B* **120**, 7737 (2016).
- [28] A. R. Young-Gonzales and R. Richert, *The Journal of Chemical Physics* **145**, 074503 (2016).
- [29] A. Young-Gonzales, K. Adrjanowicz, M. Paluch, and R. Richert, *The Journal of chemical physics* **147**, 224501 (2017).
- [30] N. J. English and J. MacElroy, *The Journal of chemical physics* **119**, 11806 (2003).
- [31] P. Marracino, A. Paffi, and G. d’Inzeo, *Physical Chemistry Chemical Physics* **24**, 11654 (2022).
- [32] D. V. Matyushov, *The Journal of Chemical Physics* **142**, 244502 (2015).
- [33] T. Samanta and D. V. Matyushov, *Journal of Molecular Liquids* **364**, 119935 (2022).
- [34] D. V. Matyushov, *RSC advances* **13**, 31123 (2023).
- [35] M. A. Sauer, T. Colburn, S. Maiti, M. Heyden, and D. V. Matyushov, *The Journal of Physical Chemistry Letters* **15**, 5420 (2024).
- [36] M. Hénot, P.-M. Déjardin, and F. Ladieu, *Phys. Chem. Chem. Phys.* **25**, 29233 (2023).
- [37] R. Chelli, P. Procacci, G. Cardini, R. Della Valle, and S. Califano, *Physical Chemistry Chemical Physics* **1**, 871 (1999).
- [38] J. Blicke, F. Affouard, P. Bordat, A. Lerbret, and M. Descamps, *Chemical Physics* **317**, 253 (2005).
- [39] A. Egorov, A. Lyubartsev, and A. Laaksonen, *The Journal of Physical Chemistry B* **115**, 14572 (2011).
- [40] M. Becher, T. Wohlfromm, E. Rössler, and M. Vogel, *The Journal of Chemical Physics* **154**, 124503 (2021).
- [41] Due to the effect of PBCs with the Ewald summation used in the treatment of Coulomb interactions [71, 72], C_{cross} is obtained by considering only pairs of dipoles closer than 7.5 Å, see ref. [36].
- [42] Experimentally to avoid dielectric breakdown, $E_0 < 70 \text{ MV}\cdot\text{m}^{-1}$ [74]. Such fields are too weak to resolve non-linear effects in the simulation due to the limited system size and simulation time. At 263 K, the maximum field we used was $190 \text{ MV}\cdot\text{m}^{-1}$ for which small deviations from linearity start to be perceptible on $C(0)$. We thus determined κ and λ at this temperature by a fit on $E_0 < 114 \text{ MV}\cdot\text{m}^{-1}$.
- [43] P. Zarzycki and B. Gilbert, *Physical Chemistry Chemical Physics* **22**, 1011 (2020).
- [44] E. Thoms, D. V. Matyushov, and R. Richert, *The Journal of Chemical Physics* **156**, 171102 (2022).
- [45] J. P. Gabriel, P. Zourchang, F. Pabst, A. Helbling, P. Weigl, T. Böhmer, and T. Blochowicz, *Physical Chemistry Chemical Physics* **22**, 11644 (2020).
- [46] K. Koperwas and M. Paluch, *Physical Review Letters* **129**, 025501 (2022).
- [47] F. Alvarez, A. Arbe, and J. Colmenero, *The Journal of Chemical Physics* **159**, 134505 (2023).
- [48] D. V. Matyushov and R. Richert, *The Journal of Physical Chemistry Letters* **14**, 4886 (2023).
- [49] P. M. Déjardin, W. T. Coffey, F. Ladieu, and Y. P. Kalmykov, Nonlinear dielectric relaxation in ac and dc electric fields, in *Nonlinear Dielectric Spectroscopy*, edited by R. Richert (Springer International Publishing, Cham, 2018) pp. 35–74.
- [50] L. Berthier and G. Biroli, *Rev. Mod. Phys.* **83**, 587 (2011).
- [51] S. Sastry, *PhysChemComm* **3**, 79 (2000).
- [52] C. Alba-Simionesco, D. Kivelson, and G. Tarjus, *The Journal of chemical physics* **116**, 5033 (2002).
- [53] C. Dalle-Ferrier, C. Thibierge, C. Alba-Simionesco, L. Berthier, G. Biroli, J.-P. Bouchaud, F. Ladieu, D. L’Hôte, and G. Tarjus, *Physical Review E* **76**, 041510 (2007).
- [54] P. Lunkenheimer and A. Loidl, *Chemical Physics* **284**, 205 (2002).
- [55] F. Ritort and P. Sollich, *Advances in physics* **52**, 219 (2003).
- [56] D. Chandler and J. P. Garrahan, *Annual review of physical chemistry* **61**, 191 (2010).
- [57] R. N. Chacko, F. P. Landes, G. Biroli, O. Dauchot, A. J. Liu, and D. R. Reichman, *Physical Review Letters* **127**, 048002 (2021).
- [58] M. R. Hasyim and K. K. Mandadapu, *Proceedings of the National Academy of Sciences* **121**, e2322592121 (2024).
- [59] J. C. Dyre, *The Journal of Physical Chemistry Letters* **15**, 1603 (2024).
- [60] X. Xia and P. G. Wolynes, *Proceedings of the National Academy of Sciences* **97**, 2990 (2000).
- [61] J.-P. Bouchaud and G. Biroli, *The Journal of chemical physics* **121**, 7347 (2004).
- [62] P. Kim, A. R. Young-Gonzales, and R. Richert, *The Journal of Chemical Physics* **145**, 064510 (2016).
- [63] T. Speck, *The Journal of Chemical Physics* **155**, 014506 (2021).
- [64] F. Ladieu, C. Brun, and D. L’Hôte, *Physical Review B* **85**, 184207 (2012).
- [65] U. Buchenau, *The Journal of Chemical Physics* **146**, 214503 (2017).
- [66] E. Bertin and F. Ladieu, *Physical Review E* **109**, 064156 (2024).
- [67] M. Baity-Jesi, G. Biroli, and D. R. Reichman, *The European Physical Journal E* **44**, 77 (2021).
- [68] E. Thoms, A. Grzybowski, S. Pawlus, and M. Paluch, *The Journal of Physical Chemistry Letters* **9**, 1783 (2018).
- [69] J.-P. Bouchaud, arXiv preprint arXiv:2402.01883 (2024).
- [70] A. Hamilton, *Monthly Notices of the Royal Astronomical Society* **312**, 257 (2000).
- [71] M. Neumann, *Molecular Physics* **57**, 97 (1986).
- [72] C. Zhang, J. Hutter, and M. Sprik, *The journal of physical chemistry letters* **7**, 2696 (2016).
- [73] G. Diezemann, *Physical Review E* **98**, 042106 (2018).
- [74] P. Lunkenheimer, M. Michl, T. Bauer, and A. Loidl, *The European Physical Journal Special Topics* **226**, 3157 (2017).